The unusual aspect of the present structural determinations then is the formation of the geometries for **1** and **2**, displaced toward the square or rectangular pyramid 78.7% and 60.2%, respectively. In these cases, no hydrogen bonding is present and lattice effects are not indicated to be important. For example, only one type of molecule per unit cell is found for each, while the fluorosilicate, **10**, shows two types of molecules per unit cell. Hence, we take the observed geometries of **1** and **2** as evidence supporting the ease of structural distortion in going down the periodic series from Si to Ge to Sn. VSEPR theory[36] supports this trend in that the larger, less electrongative central atom of a five-coordinated species would suffer decreased electron bond-pair repulsion. This effect favors the displacement toward the inherently less stable RP. The greater RP character for the *n*-butyl derivative, **1**, over the phenyl derivative, **2**, follows the observation that the presence of larger, less electronegative groups in the fifth position causes displacement toward the square pyramid.[17,32] These same tendencies were found to operate in the group 5 series, where molecular nonrigidity increased in the order P < As < Sb.[9,10]

Acknowledgment. The support of this research by the National Science Foundation (Grant CHE8504737) is gratefully acknowledged. We also thank the University of Massachusetts Computing Center for generous allocation of computer time.

Registry No. **1**, 113161-03-8; **2**, 113161-05-0; **3**, 113161-07-2; **4**, 113161-09-4; **5**, 113161-11-8; **6**, 113216-79-8; *n*-butyltin trichloride, 1118-46-3; sodium ethanedithiolate, 23851-16-3; phenyltin trichloride, 1124-19-2; methyltin trichloride, 993-16-8; bis(ethane-1,2-dithiolato)tin, 176-56-7.

Supplementary Material Available: Thermal parameters, hydrogen atom parameters, and additional bond lengths and angles (Tables S1–S3, respectively, for **1**, Tables S4–S6, for **2**, Tables S7–S9, for **3**, and Tables S10–S12, for **4**) and deviations from least-squares mean planes (Tables S13–S16, for **1–4**, respectively) (10 pages); tables of calculated and observed structure factors for **1–4** (31 pages). Ordering information is given on any current masthead page.

(36) Gillespie, R. J. *Molecular Geometry*; Van Nostrand: New York, 1972.

Contribution from the Department of Chemistry, University of British Columbia, Vancouver, BC, Canada V6T 1Y6

Pyrazine and Pyridine Complexes of Copper(II) Trifluoromethanesulfonate. Crystal Structure of Tetrakis(pyridine)bis(trifluoromethanesulfonato-*O*)copper(II) and Magnetic Exchange in (Pyrazine)bis(trifluoromethanesulfonato-*O*)copper(II)

John S. Haynes, Steven J. Rettig, John R. Sams, James Trotter,* and Robert C. Thompson*

Received October 30, 1987

Copper(II) trifluoromethanesulfonate reacts with excess pyridine or pyrazine to yield complexes of compositions $Cu(py)_4(CF_3SO_3)_2$ and $Cu(pyz)_4(CF_3SO_3)_2 \cdot H_2O$. Crystals of $Cu(py)_4(CF_3SO_3)_2$ are orthorhombic, of space group *Pbcn*, with $a = 10.5618$ (7) Å, $b = 16.287$ (1) Å, $c = 16.830$ (2) Å, $Z = 4$, and $R = R_w = 0.046$ for 1130 reflections with $I \geq 2\sigma(I)$. The *trans*-$Cu(py)_4(CF_3SO_3)_2$ molecule has crystallographic C_2 symmetry. The coordination about Cu is tetragonally distorted pseudooctahedral with mean Cu–N = 2.035 Å and Cu–O = 2.425 (4) Å. An analogous structure with trans-axially coordinated anions and equatorially bound monodentate pyrazine ligands is proposed for $Cu(pyz)_4(CF_3SO_3)_2 \cdot H_2O$. Thermolysis of this latter compound at 87 °C yields $Cu(pyz)(CF_3SO_3)_2$, and spectroscopic studies on this material support a sheet structure in which chains of copper atoms, doubly bridged by bidentate sulfonate groups, are cross-linked by bidentate bridging pyrazine ligands. Magnetic susceptibility studies (100–4.2 K) reveal antiferromagnetic behavior with a maximum in the susceptibility at ~7 K. Exchange coupling is considered to take place primarily via the bridging pyrazine groups; analysis of the magnetic data according to a Heisenberg linear-chain model yields best fit values of $J = -3.78$ cm^{-1} and $g = 2.08$.

Introduction

Several transition-metal complexes containing the coordinated trifluoromethanesulfonate (triflate) ligand have been synthesized in recent years;[1-3] interest in the molecular and electronic structures of these compounds, as well as in their potential as inorganic synthons, stems from the low basicity of the $CF_3SO_3^-$ anion and hence from its expected poor coordinating ability.[1] We report here the synthesis and characterization of 1,4-diazine (pyrazine, pyz) and azine (pyridine, py) complexes of copper(II) trifluoromethanesulfonate.[4] $Cu(pyz)_4(CF_3SO_3)_2 \cdot H_2O$ and $Cu(py)_4(CF_3SO_3)_2$ were obtained by reaction of copper(II) trifluoromethanesulfonate with an excess of the appropriate base in methanol. The pyridine complex was obtained in crystalline form, and because of the relative paucity of structural data on transition-metal complexes containing coordinated triflate,[1] a single-crystal X-ray study was undertaken on this compound. Thermolysis of the tetrakis(pyrazine) complex gave $Cu(pyz)(CF_3SO_3)_2$; this compound is of particular interest because of the opportunity for pyrazine bridging as in the nitrate[5] and hexafluoroacetylacetonate[6] analogues and the consequent possibility of magnetic exchange between metal centers. Exchange was observed previously for the nitrate but not for the hexafluoroacetylacetonate.

Experimental Section

Synthesis. Tetrakis(pyridine)bis(trifluoromethanesulfonato-*O*)copper(II), $Cu(py)_4(CF_3SO_3)_2$. Copper(II) trifluoromethanesulfonate[4] (0.994 g, 2.75 mmol) was dissolved in hot methanol (11 mL). An excess of pyridine (5 mL, 62 mmol) was added dropwise, whereupon an intensely blue solution formed. On cooling, a blue crystalline solid resulted, which was isolated by filtration. The product was recrystallized from a solution of pyridine in methanol (1:4 v/v) and isolated in 82% yield. Anal. Calcd for $CuC_{22}H_{20}N_4F_6S_2O_6$: C, 38.97; H, 2.97; N, 8.26. Found: C, 38.99; H, 2.97; N, 8.29.

Tetrakis(pyrazine)bis(trifluoromethanesulfonato-*O*)copper(II) Hydrate, $Cu(pyz)_4(CF_3SO_3)_2 \cdot H_2O$. Copper(II) trifluoromethanesulfonate (0.565 g, 1.55 mmol) was dissolved in hot methanol (3 mL). The copper(II) solution was then added to a hot solution of pyrazine (1.781 g, 22.3 mmol) dissolved in methanol (5 mL). A dark blue solution resulted, and after a period of 30 min, a blue crystalline solid formed; the product was isolated by filtration in 92% yield. Anal. Calcd for $CuC_{18}H_{18}N_8F_6S_2O_7$: C, 30.88; H, 2.59; N, 16.01. Found: C, 30.65; H, 2.57; N, 15.75.

(Pyrazine)bis(trifluoromethanesulfonato-*O*)copper(II), $Cu(pyz)(CF_3SO_3)_2$. When $Cu(pyz)_4(CF_3SO_3)_2 \cdot H_2O$ was heated in an Aberhalden drying pistol at a temperature of 87 °C in the presence of phos-

(1) Lawrance, G. A. *Chem. Rev.* **1986**, *86*, 17.
(2) Haynes, J. S.; Rettig, S. J.; Sams, J. R.; Thompson, R. C.; Trotter, J. *Can. J. Chem.* **1986**, *64*, 429.
(3) Gill, M. S.; Sethi, A. K.; Verma, R. D. *Can. J. Chem.* **1987**, *65*, 409.
(4) Arduini, A. L.; Garnett, M.; Thompson, R. C.; Wong, T. C. T. *Can. J. Chem.* **1975**, *53*, 3812.
(5) (a) Santoro, A.; Mighell, A. D.; Reimann, C. W. *Acta Crystallogr., Sect. B: Struct. Crystallogr. Cryst. Chem.* **1970**, *B26*, 979. (b) Boyd, P. D. W.; Mitra, S. *Inorg. Chem.* **1980**, *19*, 3547.
(6) (a) Belford, R. C. E.; Fenton, D. E.; Truter, M. R. *J. Chem. Ssoc., Dalton Trans.* **1974**, 17. (b) Richardson, H. W.; Wasson, J. R.; Hatfield, W. E. *Inorg. Chem.* **1977**, *16*, 484.

0020-1669/88/1327-1237$01.50/0

Table I. Crystallographic Data[a]

compd	$Cu(py)_4(CF_3SO_3)_2$
formula	$C_{22}H_{20}CuF_6N_4O_6S_2$
fw	678.1
cryst system	orthorhombic
space group	*Pbcn*
a, Å	10.5618 (7)
b, Å	16.287 (1)
c, Å	16.830 (2)
V, Å^3	2895.0 (4)
Z	4
D_c, g/cm^3	1.556
F(000)	1372
μ(Mo Kα), cm^{-1}	9.72
cryst dimens, mm	0.13 × 0.40 × 0.51
transmission factors	0.669–0.890
scan type	ω–2θ
scan range, deg in ω	0.67 + 0.35 tan θ
scan speed, deg/min	1.1–10.0
data collected	$+h,+k,+l$
$2\theta_{max}$, deg	54
cryst decay	negligible
no. of unique reflcns	3168
no. of reflcns with $I \geq 2\sigma(I)$	1130
no. of variables	188
R	0.046
R_w	0.046
S	1.712
mean Δ/σ (final cycle)	0.02
max Δ/σ (final cycle)	0.095
residual density, e/Å^3	0.4 (near Fe)

[a] Temperature 295 K, Enraf-Nonius CAD4-F diffractometer, Mo Kα radiation ($\lambda_{K\alpha_1}$ = 0.709 30, $\lambda_{K\alpha_2}$ = 0.713 59 Å), graphite monochromator, takeoff angle 2.7°, aperture (2.0 + tan θ) × 4.0 mm at a distance of 173 mm from the crystal, scan range extended by 25% on both sides for background measurement, $\sigma^2(I) = S + 2B + [0.04(S - B)]^2$ (S = scan count, B = normalized background count), function minimized $\sum w(|F_o| - |F_c|)^2$ where $w = 1/\sigma^2(F)$, $R = \sum||F_o| - |F_c||/\sum|F_o|$, $R_w = [\sum w(|F_o| - |F_c|)^2/\sum w|F_o|^2]^{1/2}$, $S = [\sum w(|F_o| - |F_c|)^2/(m - n)]^{1/2}$. Values given for R, R_w, and S are based on those reflections with $I \geq 2\sigma(I)$.

phorus(V) oxide for 14 h in vacuo, the mono(pyrazine) complex was produced. Anal. Calcd for $CuC_6H_4N_2F_6S_2O_6$: C, 16.31; H, 0.91; N, 6.34. Found: C, 16.33; H, 1.00; N, 6.24.

Physical Measurements. Infrared and electronic spectra (Nujol mulls) and differential scanning calorimetry measurements were made by using equipment and procedures previously described.[7] Magnetic susceptibility measurements were made on powdered samples using a PAR Model 155 vibrating-sample magnetometer[8] and were corrected for the diamagnetism of all atoms. These corrections are as follows (in 10^{-6} cm^3 mol^{-1}): copper, −11; $CF_3SO_3^-$, −46; pyridine, −49; pyrazine, −45. A value of 60 × 10^{-6} cm^3 mol^{-1} was used to correct for the temperature-independent paramagnetism of copper(II). Analyses for C, H, and N were performed by P. Borda of this department.

X-ray Crystallographic Analysis of $Cu(py)_4(CF_3SO_3)_2$. Crystallographic data are presented in Table I. The final unit-cell parameters were obtained by least squares on 2(sin θ)/λ values for 25 reflections (2θ = 28–36°) measured with Mo Kα_1 radiation. The data were corrected for Lp and absorption (numerical integration).[9]

With Z = 4, the molecule is constrained by space group symmetry to have $\bar{1}$-C_i or 2-C_2 symmetry, the latter being consistent with the Patterson function from which the Cu and S coordinates were determined. The remaining non-hydrogen atoms were positioned from a subsequent difference map. In the final stages of full-matrix least-squares refinement, the non-hydrogen atoms were refined with anisotropic thermal parameters and the hydrogen atoms were fixed in idealized positions (C–H = 0.97 Å, $U_H \propto U_{bonded\ atom}$). Neutral-atom scattering factors and anomalous dispersion corrections (for Cu and S) were taken from ref 10.

Table II. Final Positional (Fractional, ×10^4; Cu and S, ×10^5) and Isotropic Thermal Parameters (U × 10^3 Å^2) with Estimated Standard Deviations in Parentheses[a]

atom	*x*	*y*	*z*	U_{eq}
Cu	50000	38590 (6)	25000	58
S	22562 (16)	38966 (11)	10286 (11)	61
F(1)	1735 (7)	4037 (5)	−477 (3)	150
F(2)	3449 (6)	3370 (3)	−200 (3)	145
F(3)	3422 (5)	4670 (3)	−100 (3)	136
O(1)	3452 (4)	3856 (3)	1436 (3)	74
O(2)	1572 (5)	4636 (3)	1183 (4)	104
O(3)	1537 (4)	3159 (3)	1041 (3)	81
N(1)	5000	5114 (4)	2500	50
N(2)	5000	2598 (4)	2500	68
N(3)	3633 (5)	3824 (3)	3338 (4)	57
C(1)	2679 (11)	4027 (5)	−20 (6)	106
C(2)	4801 (7)	5536 (4)	1838 (4)	67
C(3)	4781 (9)	6387 (4)	1824 (5)	81
C(4)	5000	6807 (5)	2500	90
C(5)	3977 (6)	2186 (4)	2268 (4)	77
C(6)	3954 (7)	1342 (4)	2248 (5)	92
C(7)	5000	918 (5)	2500	99
C(8)	3774 (6)	3416 (4)	4018 (5)	70
C(9)	2873 (9)	3322 (5)	4559 (5)	92
C(10)	1699 (9)	3684 (6)	4423 (6)	105
C(11)	1528 (7)	4102 (5)	3743 (5)	91
C(12)	2506 (7)	4177 (4)	3220 (4)	66

[a] U_{eq} = $^1/_3$(trace of diagonalized U).

Table III. Bond Lengths (Å) with Estimated Standard Deviations in Parentheses

Cu–O(1)	2.425 (4)	N(2)–C(5)	1.331 (6)
Cu–N(1)	2.045 (6)	N(3)–C(8)	1.331 (8)
Cu–N(2)	2.053 (6)	N(3)–C(12)	1.336 (7)
Cu–N(3)	2.020 (5)	C(2)–C(3)	1.386 (8)
S–O(1)	1.439 (4)	C(3)–C(4)	1.347 (8)
S–O(2)	1.428 (5)	C(5)–C(6)	1.375 (9)
S–O(3)	1.422 (4)	C(6)–C(7)	1.370 (8)
S–C(1)	1.832 (10)	C(8)–C(9)	1.326 (10)
F(1)–C(1)	1.259 (11)	C(9)–C(10)	1.392 (11)
F(2)–C(1)	1.378 (9)	C(10)–C(11)	1.343 (10)
F(3)–C(1)	1.317 (9)	C(11)–C(12)	1.363 (9)
N(1)–C(2)	1.325 (7)		

Table IV. Bond Angles (deg) with Estimated Standard Deviations in Parentheses[a]

O(1)–Cu–N(1)	90.12 (11)	Cu–N(3)–C(8)	122.3 (5)
O(1)–Cu–N(2)	89.88 (11)	Cu–N(3)–C(12)	121.4 (5)
O(1)–Cu–N(3)	91.9 (2)	C(8)–N(3)–C(12)	116.2 (6)
O(1)–Cu–O(1)′	179.8 (2)	S–C(1)–F(1)	113.4 (7)
O(1)–Cu–N(3)′	88.1 (2)	S–C(1)–F(2)	105.4 (6)
N(1)–Cu–N(2)	180	S–C(1)–F(3)	109.7 (7)
N(1)–Cu–N(3)	91.59 (15)	F(1)–C(1)–F(2)	110.1 (10)
N(2)–Cu–N(3)	88.41 (15)	F(1)–C(1)–F(3)	113.5 (9)
N(3)–Cu–N(3)′	176.8 (3)	F(2)–C(1)–F(3)	104.1 (8)
O(1)–S–O(2)	113.3 (3)	N(1)–C(2)–C(3)	122.3 (7)
O(1)–S–O(3)	115.0 (3)	C(2)–C(3)–C(4)	119.4 (7)
O(1)–S–C(1)	104.5 (4)	C(3)–C(4)–C(3)′	118.9 (8)
O(2)–S–O(3)	116.1 (3)	N(2)–C(5)–C(6)	121.7 (6)
O(2)–S–C(1)	101.6 (4)	C(5)–C(6)–C(7)	118.9 (6)
O(3)–S–C(1)	104.0 (4)	C(6)–C(7)–C(6)′	119.4 (8)
Cu–O(1)–S	160.7 (3)	N(3)–C(8)–C(9)	124.6 (6)
Cu–N(1)–C(2)	121.2 (4)	C(8)–C(9)–C(10)	118.5 (7)
C(2)–N(1)–C(2)′	117.6 (7)	C(9)–C(10)–C(11)	118.3 (8)
Cu–N(2)–C(5)	120.3 (3)	C(10)–C(11)–C(12)	119.6 (7)
C(5)–N(2)–C(5)′	119.3 (7)	N(3)–C(12)–C(11)	122.7 (6)

[a] Primed atoms have coordinates related to those in Table II by the symmetry operation $1 - x, y, {}^1/_2 - z$.

(7) Haynes, J. S.; Oliver, K. W.; Thompson, R. C. *Can. J. Chem.* **1985**, *63*, 1111.
(8) Haynes, J. S.; Oliver, K. W.; Rettig, S. J.; Thompson, R. C.; Trotter, J. *Can. J. Chem.* **1984**, *62*, 891.
(9) The computer programs used include locally written programs for data processing and locally modified versions of the following: ORFLS, full-matrix least squares, and ORFFE, function and errors, by W. R. Busing, K. O. Martin, and H. A. Levy; FORDAP, Patterson and Fourier syntheses, by A. Zalkin; ORTEP II, illustrations, by C. K. Johnson; AGNOST, absorption corrections, by J. A. Ibers; MULTAN 80, multisolution program by P. Main, S. J. Fiske, S. E. Hull, L. Lessinger, G. Germain, J. P. Declercq, and M. M. Woolfson.
(10) *International Tables for X-ray Crystallography*; Kynoch: Birmingham, England, 1974; Vol. IV, pp 99–102, 149. (Present distributor: D. Reidel, Dordrecht, Holland.)

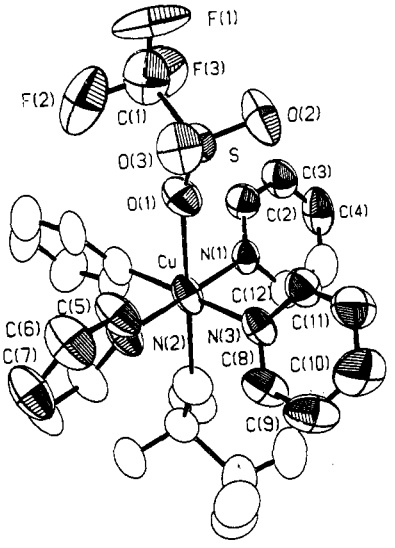

Figure 1. ORTEP plot of the structure of $Cu(py)_4(CF_3SO_3)_2$. 50% probability thermal ellipsoids are shown, and shaded atoms comprise the asymmetric unit.

Final positional and equivalent isotropic thermal parameters for the non-hydrogen atoms are given in Table II. Bond lengths and bond angles appear in Tables III and IV, respectively. Calculated hydrogen parameters, anisotropic thermal parameters, torsion angles, and structure factors are included as supplementary material.

Results and Discussion

$Cu(py)_4(CF_3SO_3)_2$. Reaction of anhydrous copper(II) trifluoromethanesulfonate with an excess of pyridine in hot methanol results, on cooling, in the precipitation of the tetrakis(pyridine) complex as a blue crystalline solid. The crystal structure analysis of $Cu(py)_4(CF_3SO_3)_2$ shows the coordination sphere around copper (Figure 1) to consist of a square-planar array of nitrogen atoms from four pyridine moieties with axial coordination sites occupied by oxygen atoms from trans-coordinated unidentate triflate anions. Unlike the situation in the analogous iron derivative, $Fe(py)_4(CF_3SO_3)_2$,[2] the coordination sphere in the copper complex is strongly distorted from regular octahedral geometry, the difference between the Cu–O (2.425 (4) Å) and mean Cu–N (2.035 Å) bond distances reflecting the large tetragonal distortion present.

$Cu(py)_4(CF_3SO_3)_2$ possesses a 2-fold axis of symmetry, but unlike the iron derivative in which the 2-fold axis bisects the cis N–Fe–N angle, the twofold axis in $Cu(py)_4(CF_3SO_3)_2$ lies along the N(1)–Cu–N(2) vector. The four nitrogen atoms and the copper atom lie in one plane, and the pyridine rings are planar within experimental error. The pyridine rings are canted out of the CuN_4 plane (56.7–64.7°) in a propeller-like arrangement as found for the iron compound. In $Cu(py)_4(CF_3SO_3)_2$, the mean Cu–N distance (2.035 Å) is typical for a Cu–N bond in which the nitrogen-containing ligand is bound in the equatorial plane. For example, the Cu–N bond distances in $Cu(pyz)_2(ClO_4)_2$[11] and $Cu(NH_3)_4SO_4\cdot H_2O$[12] are 2.06 and 2.05 Å, respectively. The Cu–O bond distances in $Cu(py)_4(CF_3SO_3)_2$ (2.425 (4) Å) and in two related structures provide for an interesting comparison. The inner coordination spheres in $Cu(pyz)_2(ClO_4)_2$[11] and $Cu(H_2O)_4(CH_3SO_3)_2$[13] are both distorted by a tetragonal elongation, and anions are weakly bonded in the axial positions; the Cu–O bond lengths are 2.373 (12) and 2.381 (8) Å for the perchlorate and methanesulfonate complexes, respectively. The longer Cu–O bond length in the triflate compound studied here, signifies a weaker cation–anion interaction in this complex, which may reflect the more weakly basic nature of the triflate anion in comparison to that of perchlorate and methanesulfonate anions.

Table V. Vibrational Spectra (Anion Bands)[a]

	IR freq, cm^{-1}		
assignt[b]	$Cu(py)_4(CF_3SO_3)_2$	$Cu(pyz)_4(CF_3SO_3)_2\cdot H_2O$	$Cu(pyz)_4(CF_3SO_3)_2$
$\nu_4(E)$	1293 s	1280 s	1310 s
	1250 s	1225 s	1209 s
$\nu_1(A_1)$	1035 s	1027 s	1030 s
$\nu_2(A_1)$	765 m	761 w	771 w
$\nu_5(E)$	525 m	521 m	528 sh
			521 m
$\nu_3(A_1)$	642 s	635 s	640 s

[a] Abbreviations: s, strong; m, medium; w, weak; sh, shoulder. [b] Assignments (CSO_3 part, C_{3v} symmetry) from ref 14.

The bonding parameters for the triflate anion are similar to those found for $Fe(py)_4(CF_3SO_3)_2$.[2] For example, the triflate anion adopts a staggered-ethane configuration about the S–C bond and the O–S–O angles are greater than the C–S–O angles. The S–O bond lengths are similar to those found in $Fe(py)_4(CF_3SO_3)_2$, the S–O(1) bond involving the oxygen bound to copper, 1.439 (4) Å, being longer than those involving the terminally bound oxygen atoms, mean 1.425 (3) Å.

The spectroscopic and magnetic properties of $Cu(py)_4(CF_3SO_3)_2$ are consistent with its molecular structure. In the infrared spectrum, the 8a and 16b vibrations of pyridine are at 1607 and 443 cm^{-1}, respectively, showing the expected shifts to higher frequencies on coordination.[2] Bands assignable to the CSO_3 part of the anion (Table V) give evidence for reduction in symmetry below C_{3v}, as expected for monodentate sulfonate coordination. In C_{3v} symmetry, two SO_3 stretching modes, $\nu_4(E)$ and $\nu_2(A_1)$, and two SO_3 deformation modes, $\nu_3(A_1)$ and $\nu_5(E)$ are expected. Although no splitting is observed in ν_5, ν_4 is split by 43 cm^{-1} (Table V). The electronic spectrum of the complex shows a broad absorption with a maximum at 17.4×10^3 cm^{-1}. The maximum is at slightly higher energy than observed for related $Cu(py)_4(RSO_3)_2$ complexes (17.2×10^3 cm^{-1} for R = F, 16.9×10^3 cm^{-1} for R = p-$CH_3C_6H_4SO_3$, 16.8×10^3 cm^{-1} for R = CH_3),[15,16] suggesting greater tetragonality in the triflate complex.[15] The magnetic moment of the complex was measured at low temperatures and found to vary from 1.84 μ_B at 61 K to 1.87 μ_B at 10 K. The magnitude of the moment and its relatively small dependence on temperature are consistent with magnetically dilute copper(II), as expected from the determined molecular structure.

Thermal analysis of $Cu(py)_4(CF_3SO_3)_2$ by differential scanning calorimetry (DSC) shows two endothermic events at 236 and 247 °C acompanied by a total weight loss of ~20%, close to that expected (~23%) for the removal of two pyridine ligands. Exothermic decomposition of the compound begins at approximately 307 °C.

$Cu(pyz)_4(CF_3SO_3)_2\cdot H_2O$. Reaction of $Cu(CF_3SO_3)_2$ with an excess of pyrazine in hot methanol yields the tetrakis(pyrazine) monohydrate as a blue powder. The presence of water of hydration is indicated by both the microanalysis and the infrared spectrum, which shows a broad absorption at 3400 cm^{-1}. Bands in the infrared spectrum that are assignable to the triflate anion are practically identical in intensity and energy with those of the pyridine analogue (Table V), thus supporting an equivalent structure with trans-axially coordinated anions and equatorially bound monodentate pyrazine ligands. It should be possible to confirm the presence of monodentate pyrazine from the IR spectrum;[17] unfortunately, the anion bands obscure much of the critical region of pyrazine absorptions. Nonetheless, strong bands at 805, 460, and 453 cm^{-1}, corresponding to the bands at 804 and 417 cm^{-1} in liquid pyrazine and to the bands at 846, 813, 494,

(11) Darriet, J.; Haddad, M. S.; Duesler, E. N.; Hendrickson, D. N. *Inorg. Chem.* **1979**, *18*, 2679.
(12) Maggi, F. *Acta Crystallogr.* **1958**, *8*, 137.
(13) Charbonnier, F.; Faure, R.; Loiseleur, H. *Acta Crystallogr., Sect. B: Struct. Crystallogr. Cryst. Chem.* **1978**, *B34*, 1504.
(14) Burger, H.; Burczyk, K.; Blaschette, A. *Monatsh. Chem.* **1970**, *101*, 102.
(15) Alleyne, C. S.; Thompson, R. C. *Can. J. Chem.* **1974**, *52*, 3218.
(16) Haynes, J. S.; Rettig, S. J.; Sams, J. R.; Thompson, R. C.; Trotter, J. *Can. J. Chem.* **1987**, *65*, 420.
(17) Goldstein, M.; Unsworth, W. D. *Spectrochim. Acta, Part A* **1971**, *27A*, 1055.

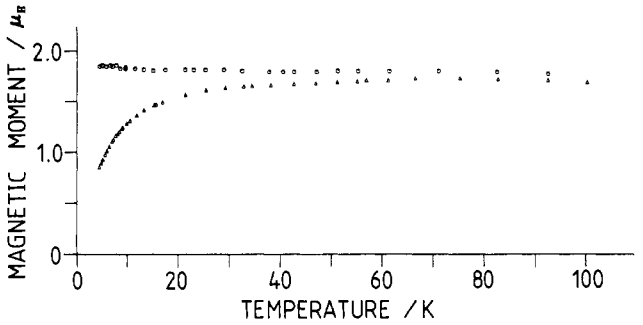

Figure 2. Plot of magnetic moment versus temperature for $Cu(pyz)_4(CF_3SO_3)_2 \cdot H_2O$ (upper) and $Cu(pyz)(CF_3SO_3)_2$ (lower).

and 440 cm^{-1} in $Cu(pyz)_2(CH_3SO_3)_2$,[16] were observed. The electronic spectrum of the complex shows a broad absorption at 16.1×10^3 cm^{-1}, a value lower than that of the pyridine analogue and consistent with a lesser degree of tetragonality, as expected considering the relative base strengths of pyridine and pyrazine. The magnetic moment varies from 1.78 μ_B at 82 K to 1.85 μ_B at 4.3 K, behavior not inconsistent with the proposed structure. Differential scanning calorimetry studies reveal endothermic events at 125 and 187 °C with a total weight loss of ~36%. This compares favorably with the calculated weight loss of ~37% for the loss of one water and three pyrazine moieties. No further thermal events occur up to ~377 °C where exothermic decomposition begins. These results indicate a high thermal stability for $Cu(pyz)(CF_3SO_3)_2$ and suggested to us the possibility of obtaining the mono(pyrazine) complex on a preparative scale by thermolysis of the tetrakis(pyrazine) compound.

$Cu(pyz)(CF_3SO_3)_2$. This compound was obtained as a pale blue powder by heating $Cu(pyz)_4(CF_3SO_3)_2 \cdot H_2O$ at 87 °C under vacuum for several hours. We were unable to obtain this complex in a form suitable for single-crystal X-ray diffraction studies; hence, our structural conclusions are based on spectroscopic evidence. The infrared spectrum (Table V) indicates the presence of only one type of anion with C_s or C_i symmetry for the CSO_3 group. Such symmetry reduction may arise through monodentate coordination as discussed above for the other complexes or through bidentate coordination involving two of the three oxygen atoms on each anion. The latter seems most likely for this compound, the difference in bonding mode accounting for the greater splitting of ν_4 compared to that observed for the other two complexes. Support for this conclusion comes from earlier work on fluorosulfates, where in $(CH_3)_2Sn(FSO_3)_2$, for example, the degree of splitting of the ν_4 band has been correlated with bidentate anion coordination.[18,19] In $Cu(pyz)(CF_3SO_3)_2$ the expected six-coordination of copper is then achieved through the presence of two bidentate anions and a bridging bidentate pyrazine ligand to give a CuN_2O_4 chromophore. Strong infrared bands at 813 and 504 cm^{-1} are readily assigned to these bridging pyrazine ligands. The electronic spectrum of $Cu(pyz)(CF_3SO_3)_2$ consists of a single broad absorption band at 13.9×10^3 cm^{-1}. The much lower energy of this band compared to the values observed for the other complexes studied in this work is consistent with the change in chromophore. The DSC results show no thermal events up to the onset of exothermic decomposition at 377 °C, as expected from the studies on the tetrakis(pyrazine) precursor.

The magnetic moment of $Cu(pyz)(CF_3SO_3)_2$ shows a significant temperature dependence; at room temperature the magnetic moment is 1.9 μ_B and this decreases to 1.7 μ_B at 100 K; at 4.2 K the moment is reduced further to 0.85 μ_B. The temperature dependence of the moment is shown in Figure 2, along with the plot for the magnetically dilute complex $Cu(pyz)_4(CF_3SO_3)_2 \cdot H_2O$ for comparison. The magnetic susceptibility (Figure 3) increases with decreasing temperature until a maximum is observed at approximately 7 K. Below this temperature, down to 4.2 K, the magnetic susceptibility decreases. These temperature dependencies of μ_{eff} and χ_m are clearly a consequence of antiferromagnetic exchange interactions propagated through the bridging ligands.

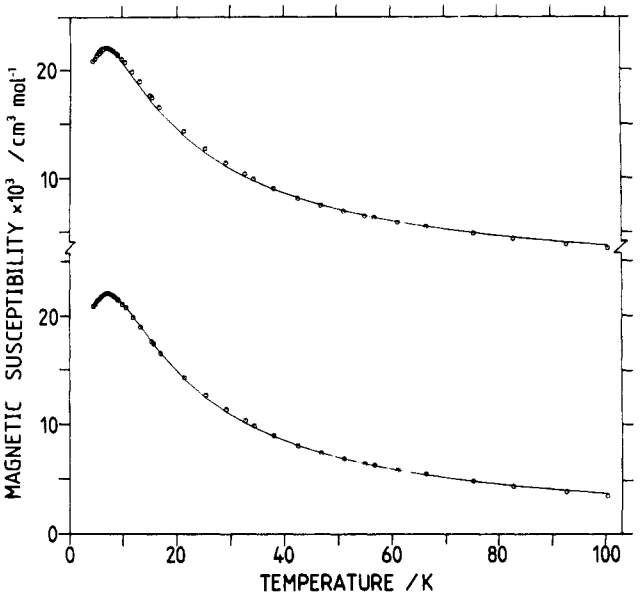

Figure 3. Plot of magnetic susceptibility versus temperature for $Cu(pyz)(CF_3SO_3)_2$. Upper: fit of data to the two-dimensional model; solid line generated for $J = -2.43$ cm^{-1}, $g = 2.10$. Lower: fit of data to linear-chain model; solid line generated for $J = -3.78$ cm^{-1}, $g = 2.08$.

Although the structure of this complex is not known, the compound almost certainly contains bridging pyz ligands and the triflate ions are also likely bridging since this is a common mode of bidentate coordination for this entity.[1] A possible structure for this material involves a square array of copper ions bridged in one dimension by double sulfonate bridges and in the other by pyrazine. This structure is analogous to that proposed for $Fe(pyz)Cl_2$.[20] The magnetic susceptibility data for the triflate derivative and for $Cu(pyz)_2(CH_3SO_3)_2$[16] exhibit similar temperature dependencies, which suggests that the dominant magnetic exchange pathway may be similar in both compounds. Considering this possibility, the Lines two-dimensional antiferromagnetic Heisenberg model[21] for spin $S = {}^1/_2$ was employed to represent the magnetic susceptibility data of $Cu(pyz)(CF_3SO_3)_2$, and the best fit[22] is represented by the solid line in Figure 3, which was generated from the following parameters: $J = -2.43$ cm^{-1}, $g = 2.10$ ($F = 0.0216$).

The susceptibility data for $Cu(pyz)_2(CH_3SO_3)_2$[16] were analyzed equally as well by using an antiferromagnetic Heisenberg ($S = {}^1/_2$) one-dimensional linear-chain model; this was explained by the presence of two inequivalent exchange pathways through pyrazine. From the proposed structure for the triflate compound, it is clear that there are at least two distinct pathways for magnetic exchange, one route through bridging pyrazine rings and the second route through bridging triflate anions. These pathways are unlikely to be equivalent, and indeed, the magnetic properties of the mono(pyrazine) derivative are also successfully represented by the linear-chain model.[23] The parameters obtained with this model are as follows: $J = -3.78$ cm^{-1}, $g = 2.08$ ($F = 0.0126$).

(18) Yeats, P. A.; Sams, J. R.; Aubke, F. *J. Chem. Soc., Chem. Commun.* **1969**, 791.
(19) Allen, F. H.; Lerbscher, J. A.; Trotter, J. *J. Chem. Soc. A* **1971**, 2507.
(20) Haynes, J. S.; Sams, J. R.; Thompson, R. C. *Inorg. Chem.* **1986**, *25*, 3740.
(21) Lines, M. E. *J. Phys. Chem. Solids* **1970**, *31*, 101.
(22) A least-squares fitting procedure allows both J and g to vary until a minimum value is obtained for the function F

$$F = \left[\frac{1}{n} \sum \left(\frac{\chi_i^{calcd} - \chi_i^{obsd}}{\chi_i^{obsd}} \right)^2 \right]^{1/2}$$

where n is the number of data points and χ_i^{obsd} and χ_i^{calcd} are the experimental and calculated molar magnetic susceptibilities.
(23) Estes, W. E.; Hatfield, W. E.; Van Oijen, J. A. C.; Reedijk, J. *J. Chem. Soc., Dalton Trans.* **1980**, 2121.

The best fit is shown as the solid line in Figure 3. In fact, for $Cu(pyz)(CF_3SO_3)_2$, the fit of the magnetic susceptibility data to the one-dimensional model is slightly improved over that for the two-dimensional model, as measured by the relative values of F and judged visually. The similarity between the magnetic properties of $Cu(pyz)(CF_3SO_3)_2$ and $Cu(pyz)_2(CH_3SO_3)_2$ suggests that the feature common to both complexes is strongly bridging pyrazine groups along one dimension. These groups provide a more facile route for magnetic exchange interactions than the other bridging entities (the axial pyrazine groups in $Cu(pyz)_2(CH_3SO_3)_2$ and the triflate anions in $Cu(pyz)(CF_3SO_3)_2$).

Acknowledgment. We thank the Natural Sciences and Engineering Research Council of Canada for financial support and the University of British Columbia Computing Centre for assistance. J.S.H. thanks the UBC Graduate Scholarship Committee for scholarship awards.

Registry No. $Cu(py)_4(CF_3SO_3)_2$, 113110-58-0; $Cu(pyz)_4(CF_3SO_3)_2 \cdot H_2O$, 113110-59-1; $Cu(pyz)(CF_3SO_3)_2$, 113110-61-5.

Supplementary Material Available: Listings of calculated hydrogen parameters, anisotropic thermal parameters, and torsion angles (4 pages); a table of calculated and observed structure factors (14 pages). Ordering information is given on any current masthead page.

Contribution from the Departments of Chemistry, University of Georgia, Athens, Georgia 30602, and Oklahoma State University, Stillwater, Oklahoma 74078

Dialkylamino Phosphorus Metal Carbonyls. 6. Chemistry of (Tris(diisopropylamino)triphosphine)diiron Hexacarbonyl Derivatives Including the Synthesis and Structure of Heterometallic Derivatives[1-4]

R. B. King,*† F.-J. Wu,† and E. M. Holt‡

Received August 7, 1987

Reactions of the triphosphine complex $(i\text{-Pr}_2NP)_3Fe_2(CO)_6$ with hydrogen halides (HX) result in selective cleavage of the diisopropylamino group attached to the center phosphorus atom to give orange $(i\text{-Pr}_2NP)_2P(X)Fe_2(CO)_6$ (X = Cl, Br). The complex $(i\text{-Pr}_2NP)_3Fe_2(CO)_6$ reacts similarly with the boiling alcohols ROH (R = Me, Et) in the presence of catalytic acetic acid to give orange $(i\text{-Pr}_2NP)_2P(OR)Fe_2(CO)_6$. Reduction of $(i\text{-Pr}_2NP)_2P(Cl)Fe_2(CO)_6$ with $NaBH_4$ in tetrahydrofuran solution gives yellow $(i\text{-Pr}_2NP)_2P(H)Fe_2(CO)_6$. However, reduction of $(i\text{-Pr}_2NP)_2P(H)Fe_2(CO)_6$ with $LiAlH_4$ results in phosphorus–phosphorus bond cleavage to give yellow $(i\text{-Pr}_2NPH)_2Fe_2(CO)_6$. Reactions of $(i\text{-Pr}_2NP)_2P(Cl)Fe_2(CO)_6$ with $(THF)Cr(CO)_5$ and with $NaMn(CO)_5$ give orange $(i\text{-Pr}_2NP)_2P(Cl)[Cr(CO)_5]Fe_2(CO)_6$ and red $(i\text{-Pr}_2NP)_2P[Mn(CO)_5]Fe_2(CO)_6$, respectively. An X-ray diffraction study of $(i\text{-Pr}_2NP)_2P(Cl)[Cr(CO)_5]Fe_2(CO)_6$ (monoclinic, $P2_1/c$; a = 10.222 (6) Å, b = 33.576 (29) Å, c = 10.577 (6) Å, β = 112.25 (4)°, Z = 4) indicates coordination of the distorted tetrahedral center phosphorus of the triphosphine chain to a $Cr(CO)_5$ fragment (Cr–P = 2.341 (12) Å). A similar X-ray diffraction structure of $(i\text{-Pr}_2NP)_2P[Mn(CO)_5]Fe_2(CO)_6$ (monoclinic, $P2_1/c$; a = 13.200 (3) Å, b = 13.972 (2) Å, c = 17.855 (9) Å, β = 93.82(3)°, Z = 4) indicates σ-bonding of the pyramidal center of the triphosphine chain to an $Mn(CO)_5$ group (Mn–P = 2.492 (3) Å). Reactions of $(i\text{-Pr}_2NP)_2P(H)Fe_2(CO)_6$ with $(THF)Cr(CO)_5$ and with $Fe_2(CO)_9$/THF gives orange $(i\text{-Pr}_2NP)_2P(H)[Cr(CO)_5]Fe_2(CO)_6$ and orange $(i\text{-Pr}_2NP)_2P(H)[Fe(CO)_4]Fe_2(CO)_6$, respectively, in which the center phosphorus atom of the triphosphine chain is bonded to the $M(CO)_n$ fragment (M = Cr, n = 5; M = Fe, n = 4).

Introduction

Recent results from our laboratory[4,5] have shown that the reaction of $i\text{-Pr}_2NPCl_2$ with $Na_2Fe(CO)_4$ in tetrahydrofuran solution provides a source of the (tris(diisopropylamino)triphosphine)hexacarbonyldiiron complex $(i\text{-Pr}_2NP)_3Fe_2(CO)_6$ (I) in ~30% yield, thereby making this complex readily available in ~30-g quantities. This complex is of interest because the rigid $P_2Fe_2(CO)_6$ framework holds the center phosphorus atom in an unusual environment as indicated by the unusual low-field chemical shift (δ 292.2) relative to those of phosphorus atoms in other systems not involved in multiple bonding. Furthermore, the selective acid cleavage of the diisopropylamino group bonded to the center phosphorus atom without disturbing the diisopropylamino groups bonded to the two terminal phosphorus atoms of the triphosphine chain makes $(i\text{-Pr}_2NP)_3Fe_2(CO)_6$ (I) a versatile precursor to other (triphosphine)hexacarbonyldiiron derivatives, mainly species of the general formula $(i\text{-Pr}_2NP)_2P(X)Fe_2(CO)_6$ (II). This paper presents details of our studies on (triphosphine)hexacarbonyldiiron complexes of this and related types.

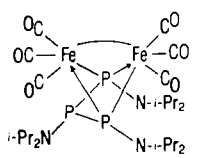

I

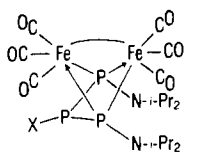

II

Our work in this area includes a study of the following two different approaches to bonding a second metal carbonyl moiety, not necessarily an iron carbonyl moiety, to the center phosphorus atom in such triphosphine complexes: (1) coordination of a suitably unhindered central phosphorus atom to a suitable transition metal fragment such as $Cr(CO)_5$ or $Fe(CO)_4$; (2) nucleophilic substitution of the halogen atom in $(i\text{-Pr}_2NP)_2P(Cl)Fe_2(CO)_6$ (II, X = Cl) with a metal carbonyl anion, namely $Mn(CO)_5^-$. This paper includes details of structure determinations by X-ray diffraction on prototypical heterometallic compounds of each type, namely $(i\text{-Pr}_2NP)_2P(Cl)[Cr(CO)_5]Fe_2(CO)_6$ (III) and $(i\text{-Pr}_2NP)_2P[Mn(CO)_5]Fe_2(CO)_6$ (IV).

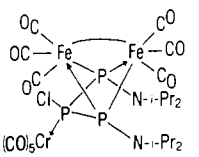

III

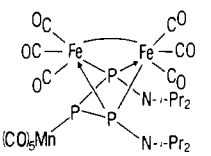

IV

Experimental Section

The general techniques for microanalyses; infrared spectra (Table I); phosphorus-31 (Table II), carbon-13 (Table III), and proton (Table IV) NMR spectra; melting points; solvent purification; and inert-atmosphere

† University of Georgia.
‡ Oklahoma State University.

(1) Part 5: King, R. B.; Wu, F.-J.; Holt, E. M. *J. Am. Chem. Soc.*, in press.
(2) This work was taken in part from: Wu, F.-J. Doctoral Disseration, University of Georgia, 1987.
(3) Portions of this work were presented at the 193rd National Meeting of the American Chemical Society, Denver, CO, April 1987.
(4) For a preliminary communication of a portion of this work, see King, R. B.; Wu, F.-J.; Holt, E. M. *Inorg. Chem.* **1986**, *25*, 1733.
(5) King, R. B.; Wu, F.-J.; Holt, E. M. *J. Am. Chem. Soc.* **1987**, *109*, 7764.

0020-1669/88/1327-1241$01.50/0